

Landscape of an exact energy functional

Aron J. Cohen

Department of Chemistry, Lensfield Rd, University of Cambridge, Cambridge, CB2 1EW, United Kingdom

Paula Mori-Sánchez

*Departamento de Química and Instituto de Física de la Materia Condensada (IFIMAC),**Universidad Autónoma de Madrid, 28049, Madrid, Spain*

(Received 17 September 2015; published 26 April 2016)

One of the great challenges of electronic structure theory is the quest for the exact functional of density functional theory. Its existence is proven, but it is a complicated multivariable functional that is almost impossible to conceptualize. In this paper the asymmetric two-site Hubbard model is studied, which has a two-dimensional universe of density matrices. The exact functional becomes a simple function of two variables whose three-dimensional energy landscape can be visualized and explored. A walk on this unique landscape, tilted to an angle defined by the one-electron Hamiltonian, gives a valley whose minimum is the exact total energy. This is contrasted with the landscape of some approximate functionals, explaining their failure for electron transfer in the strongly correlated limit. We show concrete examples of pure-state density matrices that are not v representable due to the underlying nonconvex nature of the energy landscape. The exact functional is calculated for all numbers of electrons, including fractional, allowing the derivative discontinuity to be visualized and understood. The fundamental gap for all possible systems is obtained solely from the derivatives of the exact functional.

DOI: [10.1103/PhysRevA.93.042511](https://doi.org/10.1103/PhysRevA.93.042511)

In 1964 Hohenberg and Kohn [1] established density functional theory (DFT) showing that the electron density ρ is all that is necessary to determine the exact energy of many-electron systems. However, all the challenge of electronic structure is then moved into an unknown universal functional of the density $\mathcal{F}[\rho]$. For a wave function Ψ_v that is the ground-state solution of the Schrödinger equation with potential v ,

$$E_v = \min_{\Psi} \langle \Psi | \hat{H} | \Psi \rangle = \langle \Psi_v | \hat{T} + \hat{V}_{ee} | \Psi_v \rangle + \text{Tr}(\rho_v v) \quad (1)$$

simply subtracting off the one-electron term, gives the exact Hohenberg-Kohn functional for ρ_v ($\Psi_v \rightarrow \rho_v$),

$$\mathcal{F}^{\text{HK}}[\rho_v] = E_v - \text{Tr}(\rho_v v) = \langle \Psi_v | \hat{T} + \hat{V}_{ee} | \Psi_v \rangle. \quad (2)$$

This procedure can be carried out for many different v , to obtain many points of the exact functional $\mathcal{F}^{\text{HK}}[\rho_v]$. A question arises of whether all possible densities are achievable. This is the problem of v representability that is addressed by the constrained search by Levy and Lieb [2,3] following earlier work by Percus [4],

$$\mathcal{F}^{\text{Levy}}[\rho] = \min_{\Psi \rightarrow \rho} \langle \Psi | \hat{T} + \hat{V}_{ee} | \Psi \rangle. \quad (3)$$

This functional is defined for all possible densities coming from a N -electron wave function, including those that are not obtainable as the ground-state solution of a Schrödinger equation (not v representable). Once the exact functional is known, the total energy is obtained by minimization only over densities,

$$E_v[\rho] = \min_{\rho} \{ \mathcal{F}[\rho] + \text{Tr}(\rho v) \}. \quad (4)$$

The exact functional of the first-order density matrix γ can be derived [2,5]

$$F^{\text{Levy}}[\gamma] = \min_{\Psi \rightarrow \gamma} \langle \Psi | \hat{V}_{ee} | \Psi \rangle, \quad (5)$$

and used similarly, where the kinetic energy term is now a known linear functional of γ ,

$$E_v[\rho] = \min_{\gamma} \{ F[\gamma] + \text{Tr}(\mathbf{T}\gamma) + \text{Tr}(v\gamma) \}. \quad (6)$$

In this paper, the nature of the exact first-order density matrix functional is revealed by considering the asymmetric two-site Hubbard model. In this universe, the fundamental equations are tractable and the exact functional becomes a visualizable three-dimensional energy landscape in the space of density matrices. We demonstrate how this one universal landscape gives the exact energy of all possible systems, for all numbers of electrons including fractional. This connected view of the functional for all density matrices makes clear the reasons for the failure of approximate functionals, and allows us to answer the questions of whether there are density matrices which are not v representable and also how the derivatives of the exact functional give the fundamental gap.

The asymmetric two-site Hubbard [6] model describes interacting electrons on a lattice of two sites that contains the physics of electron transfer and has even recently been experimentally described using two ultracold fermionic atoms [7]. It has the Hamiltonian

$$\hat{H} = -t \sum_{\sigma} (\hat{c}_{1\sigma}^{\dagger} \hat{c}_{2\sigma} + \hat{c}_{2\sigma}^{\dagger} \hat{c}_{1\sigma}) + U \sum_i \hat{n}_{i\alpha} \hat{n}_{i\beta} + \sum_{i\sigma} \epsilon_i \hat{n}_{i\sigma}, \quad (7)$$

where the site index $i = 1, 2$, spin index $\sigma = \alpha, \beta$, and the number operator is $\hat{n}_{i\sigma} = \hat{c}_{i\sigma}^{\dagger} \hat{c}_{i\sigma}$. There has been recent work on the exact functional in this model from Fuks *et al.* [8,9], Carrascal *et al.* [10], Pastor and co-workers [11,12], Requist *et al.* [13], and in other systems [14–16].

The parameters that define a particular model are the hopping between the sites t on-site energies ϵ_1/ϵ_2 and the electron-electron repulsion penalty due to double occupation of a site U . The physics is completely determined by $\Delta\epsilon =$

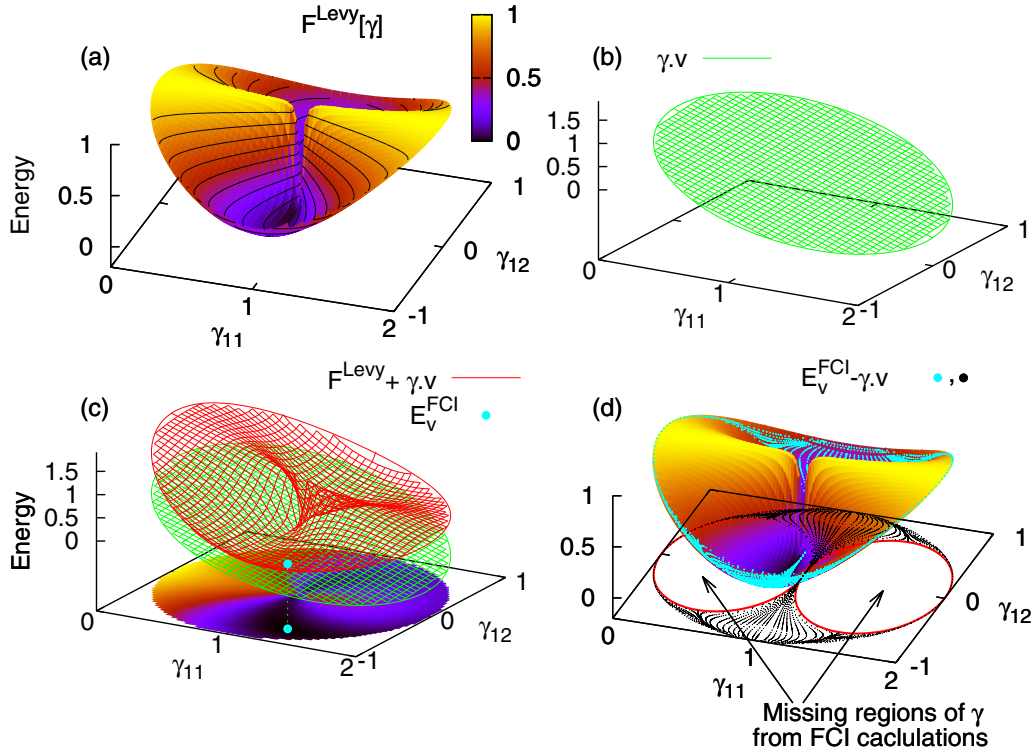


FIG. 1. Energy landscape of the exact functional (a) $F^{\text{Levy}}[\gamma]$ for all allowable density matrices of the two-site Hubbard model. (b) The one electron term $\gamma \cdot v$ for $t = 0.1$ and $\Delta\epsilon = 0.9$, which is purely a flat plane. (c) Illustration of the minimization of the exact functional adding on the same $\gamma \cdot v$ term to give the FCI energy and density matrix $\{E_v^{\text{FCI}}, \gamma_v^{\text{FCI}}\}$. (d) $F^{\text{Levy}}[\gamma]$ and 6552 points of $\{F^{\text{HK}}[\gamma_v^{\text{FCI}}, \gamma_v^{\text{FCI}}], E_v^{\text{FCI}}\}$ that show the E_v^{FCI} subtracting the one electron term [Eq. (11)] at γ_v^{FCI} for many different v .

$\epsilon_1 - \epsilon_2$ and the ratio U/t , therefore, in this work U is fixed at 1 and t and $\Delta\epsilon$ are the chosen variables. The kinetic and on-site potential part of the Hamiltonian, which together we denote as v , is a real symmetric 2×2 matrix defined by parameters t and $\Delta\epsilon$,

$$v = \begin{pmatrix} \Delta\epsilon/2 & -t \\ -t & -\Delta\epsilon/2 \end{pmatrix} \quad (8)$$

and the 2×2 density matrix $\gamma_{ij} = \sum_{\sigma} \langle \Psi | c_{i\sigma}^{\dagger} c_{j\sigma} | \Psi \rangle$ is

$$\gamma = \begin{pmatrix} \gamma_{11} & \gamma_{12} \\ \gamma_{12}^* & (2 - \gamma_{11}) \end{pmatrix} \quad (9)$$

leading to a total energy for real density matrices

$$E_v = -2\gamma_{12}t + \gamma_{11}\Delta\epsilon/2 - (2 - \gamma_{11})\Delta\epsilon/2 + F[\gamma]. \quad (10)$$

The exact functional can be obtained and understood from different perspectives. First, for any γ that comes from an exact diagonalization full configuration interaction (FCI) calculation with one-electron Hamiltonian v , the Hohenberg-Kohn functional is given by

$$F^{\text{HK}}[\gamma_v] = E_v^{\text{FCI}} + 2\gamma_{12}t - \gamma_{11}\Delta\epsilon/2 + (2 - \gamma_{11})\Delta\epsilon/2. \quad (11)$$

The second way is the constrained search over real singlet wave functions

$$\Psi = \frac{a}{\sqrt{2}}[\mathcal{A}(\phi_1\alpha\phi_2\beta) + \mathcal{A}(\phi_2\alpha\phi_1\beta)] + b\mathcal{A}(\phi_1\alpha\phi_1\beta) + c\mathcal{A}(\phi_2\alpha\phi_2\beta), \quad (12)$$

which can be simplified to an expression (see Refs. [10,12] and Supplemental Material (SM) for more details [17])

$$F^{\text{Levy}}[\gamma] = \frac{\gamma_{12}^2(1 - \sqrt{1 - \gamma_{12}^2 - [\gamma_{11} - 1]^2}) + 2[\gamma_{11} - 1]^2}{2(\gamma_{12}^2 + [\gamma_{11} - 1]^2)}. \quad (13)$$

Third, it can be viewed as the exact functional in density matrix functional theory for two electrons. From the work of Löwdin and Shull in 1956 [18] using the natural orbitals $|a\rangle$ and $|b\rangle$ ($|p\rangle = \sum_{i=1,2} C_{pi} \hat{c}_i^{\dagger} |\text{vac}\rangle$) and their occupation numbers n_a and n_b that diagonalize γ , it can be derived that

$$F^{\text{LS}}[\gamma] = \frac{1}{2}n_a\langle aa|aa\rangle + \frac{1}{2}n_b\langle bb|bb\rangle - \sqrt{n_a n_b}\langle aa|bb\rangle, \quad (14)$$

where the two-electron integral is $\langle pp|qq\rangle = U \sum_{i=1,2} C_{pi}^2 C_{qi}^2$. This gives exact agreement with the constrained search expression Eq. (13) and has been utilized in functionals such as the AGP natural orbital functional [19,20] and PNOF5 [21] (see SM [17]). There are two further possible routes to the exact functional (details in the SM [17]): the extension over pure-state wave functions to complex, and the Lieb maximization [3] $F^{\text{Lieb}}[\gamma] = \sup_v \{E_v - \gamma \cdot v\}$.

$F^{\text{Levy}}[\gamma]$ is shown in Fig. 1(a) for the allowable density matrices $(\gamma_{11} - 1)^2 + \gamma_{12}^2 \leq 1$. It is represented as a unique surface of hills and a valley in a bowl type shape, with a channel through the center (at $\gamma_{11} = 1$) and hills on both sides

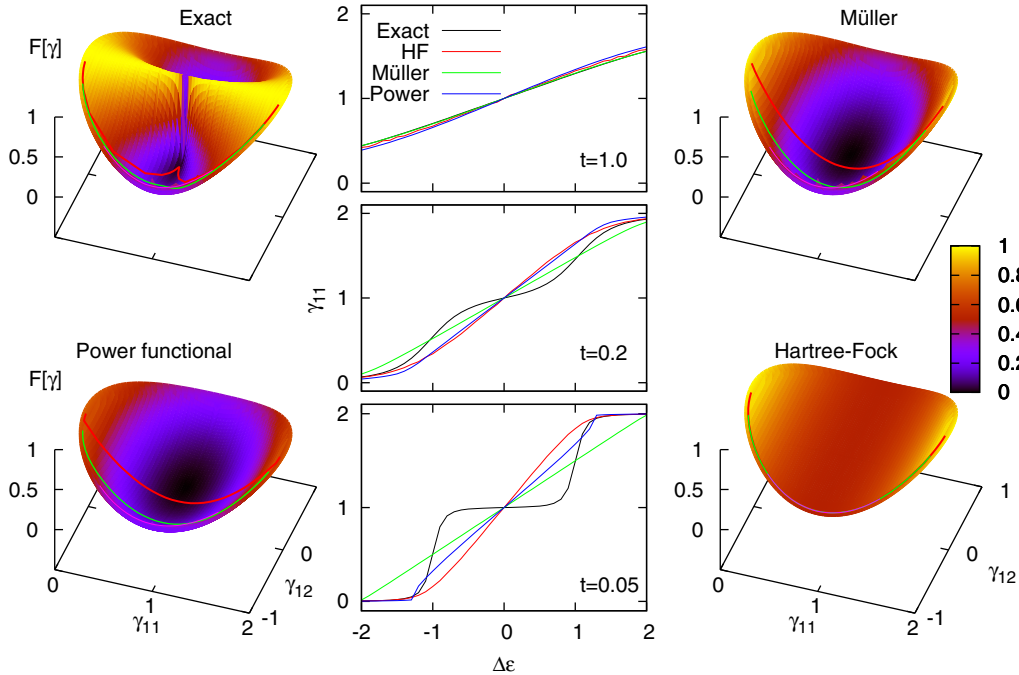


FIG. 2. Entire landscape of $F[\gamma]$ for the exact functional, and three approximate density-matrix functionals (see Supplemental Material for more details [17]). The minimizing values $\{\gamma_v, \gamma_v\}$ for three lines of v ($-2 \leq \Delta\epsilon < 2$) with $t = 1, 0.2, 0.05$ are plotted on the surfaces in purple, green, and red, respectively. The central plots show the failure of approximate functionals to correctly describe the electron transfer (γ_{11} vs $\Delta\epsilon$) as t approaches the strongly correlated limit (see supplementary animations).

(reaching 1 at $\gamma_{12} = 0$). This defines the energy landscape that maps every possible system to its corresponding exact energy.

The exact functional is an energy landscape with only one minimum, so how does it give rise to all possible FCI energies? This can be pictured in a very physical manner by considering a walk on this landscape, placed upon a flat surface tilted to the angle given by the one-electron potential, which gives a valley whose minimum equals exactly the FCI solution. Figure 1(b) shows the one electron term for a particular v , defined by $t = 0.1$ and $\Delta\epsilon = 0.9$, and Fig. 1(c) shows the addition of this with the exact functional $F^{\text{Levy}}[\gamma] + \gamma \cdot v$, whose minimum is at the FCI energy E_v^{FCI} and FCI density matrix γ_v . This holds for every possible v . Thus, once the exact functional is known, it gives the exact solution of any system by means of an almost trivial calculation.

We have performed a large number of FCI calculations varying the two free parameters, $-10 < t < 10$ and $-10 < \Delta\epsilon < 10$. Figure 1(d) illustrates the result of over 6000 FCI calculations subtracting off the one electron term $\gamma \cdot v$ to give the $F^{\text{HK}}[\gamma]$ of Eq. (11). Every single light blue dot, representing many $F^{\text{HK}}[\gamma_v]$, lies on the surface of $F^{\text{Levy}}[\gamma]$. However, the one-particle density matrices γ_v that result from all these FCI calculations cover only a small fraction of the space (seen as the black dots projected onto the base of the plot with more details in SM [17]). The rest of the density matrices are not v representable, even though they are N representable. From the perspective of the exact functional, it is clear why these density matrices can never be found, as they correspond to the hills of the surface where $F^{\text{Levy}}[\gamma]$ lies inside a convex containing surface (see SM). Addition of the one electron interaction term, which is purely linear in the variables γ_{11} and γ_{12} , as pictured in Fig. 1(b), means

that these points can never be minima, and hence cannot be a FCI solution. In terms of the functional, this corresponds to regions where the second derivatives of the functional are no longer positive definite as seen by the a negative lowest eigenvalue of the Hessian matrix of second derivatives $H_{ij} = \frac{\partial^2 F}{\partial \gamma_i \partial \gamma_j}$ (see SM). It should also be noted that the lowest energy wave functions of the non- v -representable density matrices cannot be written in a Gutzwiller form [22] (see SM). The non- v -representable region highlights the key distinction between $F^{\text{Levy}}[\gamma]$ derived from pure-state wave functions, which can be concave, versus the $F^{\text{Lieb}}[\gamma]$ functional derived from ensembles by a Legendre-Fenchel transform, which is proven to be everywhere convex [3].

The derivatives of the functional (expressions in SM) satisfy the Euler equation and give the one-electron Hamiltonian needed,

$$\frac{\partial F[\gamma]}{\partial \gamma} = -v + C. \quad (15)$$

Now, consider the physics of electron transfer by varying $\Delta\epsilon$ from the weakly correlated ($U/t = 1$) to strongly correlated ($U/t = 20$) regimes as depicted in Fig. 2. Correctly describing this electron transfer in the strongly correlated regimes is one of the great challenges of electronic structure, as demonstrated in Fig. 2 by the failure of approximate density matrix functionals such as Müller [23] and Power functionals [24]. The approximate functionals do not correctly describe the entire landscape and thus completely fail to describe electron transfer (see animation in SM). This is related to the failure of all currently used density functionals for the

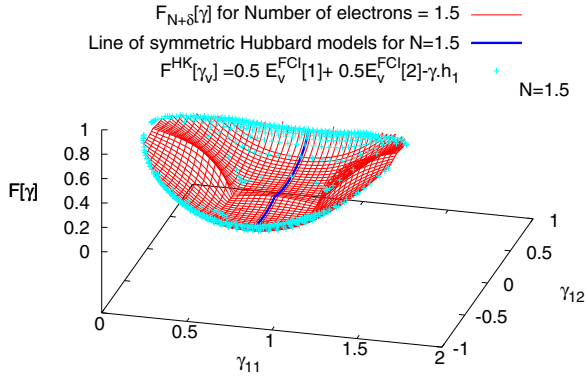


FIG. 3. The exact functionals of Eqs. (17) and (18) for $N = 1.5$ electrons, which gives back the exact energy of every system with 1.5 electrons.

electron transfer in a two-electron molecular type challenge (see $\text{HZ}^{[2e]}$ of Ref. [25]).

The exact functional can be calculated for all numbers of electrons ($0 \leq N \leq 4$); the integer parts are trivial and given in the SM. For noninteger numbers of electrons, the functional is constructed using the Perdew, Parr, Levy, and Balduz (PPLB) [26] ensemble extension to search over many-electron density matrices

$$\Gamma_{N+\delta} = c_0|\Psi_0\rangle\langle\Psi_0| + c_1|\Psi_1\rangle\langle\Psi_1| + c_2|\Psi_2\rangle\langle\Psi_2| + c_3|\Psi_3\rangle\langle\Psi_3| + c_4|\Psi_4\rangle\langle\Psi_4|, \quad (16)$$

with $\sum_i c_i = 1$ and $\sum_i c_i \cdot i = N + \delta$ ($0 \leq \delta \leq 1$). Thus we explicitly construct the fractional extension

$$F_{N+\delta}[\gamma] = \min_{\Gamma_{N+\delta} \rightarrow \gamma} \text{Tr}[\Gamma_{N+\delta} V_{ee}], \quad (17)$$

where, unlike PPLB, we have not assumed convexity of the energy versus N . That is, rather than using $\Gamma_{N+\delta} = c_N|\Psi_N\rangle\langle\Psi_N| + c_{N+1}|\Psi_{N+1}\rangle\langle\Psi_{N+1}|$, we explicitly search over ensembles of all N -electron wave functions ($N = 0, 1, 2, 3$, and 4) as in Eq. (16) (see SM).

Figure 3 shows the extension of the exact functional to fractional numbers of electrons for $N + \delta = 1.5$. We obtained $F_{N+\delta}[\gamma]$ for all the possible density matrices, where the minimum is actually given only by the combination of N and $N + 1$ (see Supplemental Material for more details [17]). We also find that all the appropriate ensembles of FCI energies subtracting off the one electron term using the ensemble of density matrices,

$$F_{N+\delta}^{\text{HK}}[v] = (1 - \delta)E_v^{\text{FCI}}[N] + \delta E_v^{\text{FCI}}[N + 1] - [(1 - \delta)\gamma_v^N + \delta\gamma_v^{N+1}] \cdot v \quad (18)$$

lie perfectly on the functional surface for all values of v and δ . Additionally, just like for integer electrons, a walk on this surface tilted to the angle of any one-electron potential [analogously to Fig. 1(c)] gives a minimum point that exactly agrees with the ensemble FCI energy.

The knowledge of the exact functional for fractional numbers of electrons connects to the band-gap problem. This is the question of whether the fundamental gap, defined as the difference of the ionization energy and electron affinity, can be given by the derivatives of the exact functional. For simplicity,

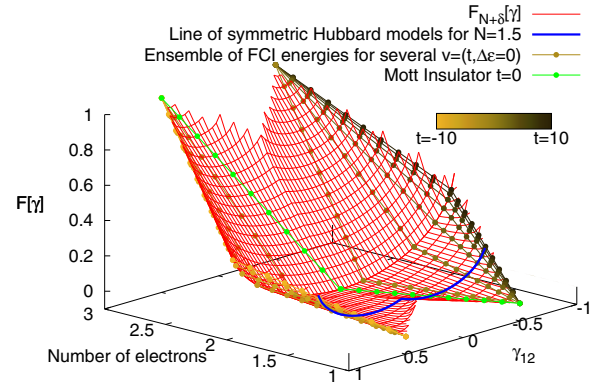


FIG. 4. The exact functionals of Eqs. (17) and (18) for all numbers of electrons ($1 \leq N \leq 3$) in the symmetric two-site Hubbard model.

consider only the symmetric Hubbard dimer with different numbers of electrons. In Fig. 4 the exact functional is shown for $1 \leq N \leq 3$, along with several points of the ensemble $F_{N+\delta}^{\text{HK}}[v]$ with $v = \{-1 < t < 1, \Delta\epsilon = 0\}$ (see also animations in SM). For every v , $F_{N+\delta}^{\text{HK}}[v]$ traces out a straight line versus particle number with a clear derivative discontinuity at $N = 2$, hence the derivatives of the exact functional give the contribution to the fundamental gap

$$\left. \frac{\partial F[\gamma]}{\partial N_+} \right|_v - \left. \frac{\partial F[\gamma]}{\partial N_-} \right|_v = F[\gamma^{N+1}] + F[\gamma^{N-1}] - 2F[\gamma^N]. \quad (19)$$

If there is no discontinuity in the density matrix, which is the case of a Mott insulator, the entirety of the fundamental gap is given by the exact functional [Eq. (19)]. This is illustrated as the green line in Fig. 4 for the symmetric Hubbard model with $t = 0$ and $1 \leq N \leq 3$, and has a direct correspondence to the gap of infinitely stretched H_2 [27]. Nevertheless, most systems have a discontinuity in the density matrix $\gamma^{N+1} - \gamma^N \neq \gamma^N - \gamma^{N-1}$, giving rise to a discontinuous derivative even for the one electron term, which is an entirely smooth flat plane. However, the direction in which γ changes upon electron addition or removal is already determined by derivatives of F while keeping the derivative in the direction of fixed N to be constant

$$\gamma_{N\pm 1} = \gamma_N + \left. \frac{\delta\gamma}{\delta N_{\pm}} \right|_{\frac{\partial F}{\partial \gamma}|_N}. \quad (20)$$

Hence, the fundamental gap is solely determined by the derivatives of the functional itself,

$$\text{Gap}[\gamma_N] = \left(\left. \frac{\partial F[\gamma]}{\partial N_+} \right|_{\frac{\partial F[\gamma]}{\partial \gamma}|_N} - \left. \frac{\partial \gamma}{\partial N_+} \right|_{\frac{\partial F}{\partial \gamma}|_N} \cdot \left. \frac{\partial F[\gamma]}{\partial \gamma} \right|_N \right) - \left(\left. \frac{\partial F[\gamma]}{\partial N_-} \right|_{\frac{\partial F[\gamma]}{\partial \gamma}|_N} - \left. \frac{\partial \gamma}{\partial N_-} \right|_{\frac{\partial F}{\partial \gamma}|_N} \cdot \left. \frac{\partial F[\gamma]}{\partial \gamma} \right|_N \right).$$

Overall, it is amazing to have a universe that turns any question about the exact functional into simple movements of a three-dimensional energy landscape. Walks on this landscape and its valley and hills correspond to important

physical concepts such as the exact energies of every possible system and domains of non- v -representable density matrices. Furthermore, in the direction of changing particle number there is a continuous surface that has a derivative discontinuity at the integers, giving all possible fundamental gaps, including Mott insulators. The whole landscape of the exact functional is itself an infinite number of exact constraints, such that any approximation must approach and be mathematically proximal to it for the entire universe. It is this connected view of the exact

functional for a family of densities in a global landscape that truly highlights a path for the improvement of approximate functionals.

We gratefully acknowledge funding from Ramón y Cajal (P.M.-S.) and the Royal Society (A.J.C.). P.M.S. also acknowledges funding from MINECO Grant No. FIS2015-64886-C5-5-P.

-
- [1] P. Hohenberg and W. Kohn, *Phys. Rev.* **136**, B864 (1964).
[2] M. Levy, *Proc. Natl. Acad. Sci. USA* **76**, 6062 (1979).
[3] E. H. Lieb, *Int. J. Quantum Chem.* **24**, 243 (1983).
[4] J. K. Percus, *Int. J. Quantum Chem.* **13**, 89 (1978).
[5] T. L. Gilbert, *Phys. Rev. B* **12**, 2111 (1975).
[6] J. Hubbard, *Proc. R. Soc. London Ser. A* **276**, 238 (1963).
[7] S. Murmann, A. Bergschneider, V. M. Klinkhamer, G. Zürn, T. Lompe, and S. Jochim, *Phys. Rev. Lett.* **114**, 080402 (2015).
[8] J. I. Fuks, M. Farzanehpour, I. V. Tokatly, H. Appel, S. Kurth, and A. Rubio, *Phys. Rev. A* **88**, 062512 (2013).
[9] J. I. Fuks and N. T. Maitra, *Phys. Chem. Chem. Phys.* **16**, 14504 (2014).
[10] D. J. Carrascal, J. Ferrer, J. C. Smith, and K. Burke, *J. Phys.: Condens. Matter* **27**, 393001 (2015).
[11] R. López-Sandoval and G. M. Pastor, *Phys. Rev. B* **66**, 155118 (2002).
[12] M. Saubanère and G. M. Pastor, *Phys. Rev. B* **84**, 035111 (2011).
[13] R. Requist and O. Pankratov, *Phys. Rev. B* **77**, 235121 (2008).
[14] A. M. Teale, S. Coriani, and T. Helgaker, *J. Chem. Phys.* **132**, 164115 (2010).
[15] S. Kvaal, U. Ekström, A. M. Teale, and T. Helgaker, *J. Chem. Phys.* **140**, 18A518 (2014).
[16] L. O. Wagner, T. E. Baker, E. M. Stoudenmire, K. Burke, and S. R. White, *Phys. Rev. B* **90**, 045109 (2014).
[17] See Supplemental Material at <http://link.aps.org/supplemental/10.1103/PhysRevA.93.042511> for background, derivations and animations of key aspects of the exact functional.
[18] P.-O. Löwdin and H. Shull, *Phys. Rev.* **101**, 1730 (1956).
[19] B. Barbiellini, *J. Phys. Chem. Solids* **61**, 341 (2000).
[20] B. Barbiellini and A. Bansil, *J. Phys. Chem. Solids* **62**, 2181 (2001).
[21] M. Piris, X. Lopez, F. Ruipérez, J. M. Matxain, and J. M. Ugalde, *J. Chem. Phys.* **134**, 164102 (2011).
[22] M. C. Gutzwiller, *Phys. Rev. Lett.* **10**, 159 (1963).
[23] A. Müller, *Phys. Lett. A* **105**, 446 (1984).
[24] S. Sharma, J. K. Dewhurst, N. N. Lathiotakis, and E. K. U. Gross, *Phys. Rev. B* **78**, 201103 (2008).
[25] P. Mori-Sánchez and A. J. Cohen, *Phys. Chem. Chem. Phys.* **16**, 14378 (2014).
[26] J. P. Perdew, R. G. Parr, M. Levy, and J. L. Balduz, Jr., *Phys. Rev. Lett.* **49**, 1691 (1982).
[27] P. Mori-Sánchez, A. J. Cohen, and W. T. Yang, *Phys. Rev. Lett.* **102**, 066403 (2009).